Seascape origin of Richards growth

Daniel W. Swartz, Bertrand Ottino-Löffler , and Mehran Kardar

Department of Physics, Massachusetts Institute of Technology, Cambridge, Massachusetts 02139, USA

First proposed as an empirical rule over half a century ago, the Richards growth equation has been frequently invoked in population modeling and pandemic forecasting. Central to this model is the advent of a fractional exponent γ, typically fitted to the data. While various motivations for this nonanalytical form have been proposed, it is still considered foremost an empirical fitting procedure. Here, we find that Richards-like growth laws emerge naturally from generic analytical growth rules in a distributed population, upon inclusion of (i) migration (spatial diffusion) among different locales, and (ii) stochasticity in the growth rate, also known as "seascape noise." The latter leads to a wide (power law) distribution in local population number that, while smoothened through the former, can still result in a fractional growth law for the overall population. This justification of the Richards growth law thus provides a testable connection to the distribution of constituents of the population.

I. INTRODUCTION

The mathematical description of growing populations has been an enduring topic of interest. There is presently a great diversity of population growth models [1–3], which have been applied in a wide variety of contexts, including epidemiology [4,5], forestry [6], developmental biology [7], cancer [2], immunology [8–11], and many others.

One such model of interest is the *Richards equation*. Originally developed as an empirical model of plant development [6,12–14], and later used as a population growth model [15], it has over the last year exploded in popularity, becoming a consistent presence in the modeling of infectious diseases, especially in COVID-19 forecasting [4,16–23].

The Richards model is described by

$$\frac{dy}{dt} = \mu y - a y^\gamma, \tag{1}$$

where y is a measure of the population size, μ is the initial growth rate (sometimes referred to as the population fitness), and a sets the final (saturation) population to $y_f = (\mu/a)^{1/(\gamma-1)}$. The feature that distinguishes this from the celebrated and more natural Verhulst logistic equation [24] is the nonanalytic (shape) parameter $\gamma > 1$. When $\gamma = 2$, a logistic equation is retrieved, but for any other value, the inflection point of the growth curve becomes off-center, leading to asymmetric growth curves, as shown in Fig. 1.

This shape parameter γ indeed gives the Richards equation character, but its meaning beyond a fitting device is mysterious. Because γ takes on fractional values, this makes the dynamics of Richards growth nonanalytic, making its origins theoretically nontrivial. Although there have been proposed derivations of Richards-like growth, they have either leaned on an underlying fractal topology [19,25,26], or relied on a detailed manipulation of an susceptible infected recovered (SIR) model, which may not be robust under model perturbation [18,27]. In practice, Richards growth is still considered an empirical law and lacks a fully universal origin, or a physically intuitive interpretation of the shape parameter γ.

In this paper, we propose a plausible origin for emergence of Richards-like growth in distributed populations from generic local analytical forms. Specifically, we shall use the *Fisher equation* as a starting point. The deterministic Fisher equation [28–32] is one of the most basic models of spatial population growth, written as

$$\frac{dy(x,t)}{dt} = \mu y - a y^2 + D\nabla^2 y. \tag{2}$$

This is distinguished from a logistic equation by the presence of a spatial coordinate x and a diffusion term D which sets the rate of local migration.

The deterministic Eq. (2) should in principle include reproductive stochasticity. While there are many kinds of randomness that may influence population growth (e.g., demographic noise, with amplitude proportional to $\sqrt{y}$ [33–38]), we are interested in what is called *seascape noise* [39–48]. This noise arises from observing that the fitness μ of a population is not necessarily a static, uniform quantity. Population fitness can vary based on minor environmental conditions, access to resources, microscopic mutation rates, and other such factors. So we generalize from a static fitness landscape $\mu(x)$ to one that varies in time $\mu(x,t)$, much as the sea surface changes in time.

By introducing seascape noise into the Fisher equation, we obtain the *seascape Fisher equation*,

$$dy = (\mu y - a y^2 + D\nabla^2 y)dt + \sigma y \, dW, \tag{3}$$

with σ^2 being the variance of the fitness noise, and $dW = dW(x,t)$ is an uncorrelated Wiener process. While our noise will be uncorrelated, we should note that in certain

applications we may wish to consider more spatially correlated environmental variations [49–52]. Moreover, we consider this stochastic differential equation under an Itô interpretation, since its assumptions pair well with the fact that generations in a population are discrete, though interesting seascape results exist for alternate interpretations [53–55]. And while interesting traveling wave solutions to equations of this type exist [28,32], we will restrict our study to initial conditions which are uniform across space.

Since both the Fisher equation and seascape noise are very versatile concepts, this makes their combination in Eq. (3) similarly adaptable. Variants of this much-studied model [56–59] have connections to the Kardar-Parisi-Zhang equation in the field of surface growth problems [60–68], the study of directed polymers in random media [56–59], symmetry breaking [69–71], theoretical ecology [35,72–76], immunology [77], and economics [78].

In this work, we argue that spatially averaging the seascape Fisher equation is sufficient to produce Richards-like growth curves. In Sec. II we introduce a discretization of the model, replacing $y(x)$ with y_i for locations (nodes) $i = 1, \ldots, N$. In the context of this model diffusion between neighboring sites can be replaced with migration between any pair of sites at rates M_{ij}. A mean-field limit is then obtained if migration rates are equal between any pair of sites ($M_{ij} = D/N$). This limit was considered by us [79] in the context of population extinction, and similar models are used by others in different contexts [69,70,77,80,81]. The steady (long-time) limit of the probability distribution $\rho(y)$ can be obtained exactly in this mean-field limit, and is characterized by a power-law distribution. A wide power-law distribution, characterized by nonanalytic dependencies of its moments, suggests a natural route for obtaining Richards-like growth. Unfortunately, we could not solve the full dynamic behavior of the model, even in the mean-field limit. As an alternative, in Sec. III we introduce a model which alternates the linear and nonlinear parts of the model. This *seasonal* growth model retains the features of seascape stochasticity and migration which we believe are the cause of Richards growth, and (with some assumptions) is exactly solvable; numerical simulations confirm these expectations. In Sec. IV we consider a number of extensions: providing a procedure for testing the model by examining the dependence of the second moment on the mean (Sec. IV A); indicating the universality of the results for generalized growth equations (Sec. IV B); numerical studies of the seascape Fisher equation in one and two dimensions (Sec. IV C); and finally indicating the appearance of Gompertz growth in the strong noise limit (Sec. IV D). The concluding Sec. V provides an overview, and outlook for future studies.

II. MEAN-FIELD STEADY STATE

The intuition for why seascape noise is a viable mechanism for Richards growth comes from earlier studies of a mean-field version of the problem. We begin with the full seascape Fisher equation Eq. (3) in d spatial dimensions. We discretize space into N lattice sites with unit spacing indexed by $i = 1, 2, \ldots, N - 1$ with periodic boundary conditions. The field $y(x, t)$ is replaced by a single value at each lattice site, $y(x = i, t) \rightarrow y_i(t)$. The Laplacian on this lattice takes the form of

a migration rate M_{ij} giving the rate of migration from site j to i. For example, on a regular one-dimensional lattice, $M_{ij} = \delta_{i+1,j} + \delta_{i-1,j} - 2\delta_{ij}$. The discretized version of the stochastic Fisher equation now takes the form

$$dy_i = \left(\mu y_i - a y_i^2 + \sum_j M_{ij} y_j \right) dt + \sigma y_i dW_i. \quad (4)$$

One can use the above equation and generalize the matrix M_{ij} to any migration connectivity network. We then proceed to take the mean-field limit by using a complete graph, defining $M_{ij} = D/N$, corresponding to a population that can migrate with "steps" of arbitrary length.

The stochastic Fisher equation in the mean-field case now takes the simple form

$$dy_i = \left(\mu y_i - a y_i^2 + D(\bar{y} - y_i) \right) dt + \sigma y_i dW_i, \quad (5)$$

where $\bar{y}$ is the spatial average of y [82]. The steady state (long-time) behavior of this stochastic ordinary differential equation is obtained as the stationary solution of a corresponding Fokker-Planck equation (see Ref. [79] and Sec. III A), and is proportional to

$$\rho(y) \propto e^{-c_D \bar{y}/y} y^{-2 - c_D + c_\mu} e^{-c_a y}, \quad (6)$$

where $c_D = 2D/\sigma^2$, $c_\mu = 2\mu/\sigma^2$, $c_a = 2a/\sigma^2$. In the limit $N \rightarrow \infty$ we can identify $\bar{y} = \langle y \rangle$ as a parameter to be found self-consistently [69,70,79–81,83]. The steady state distribution thus has a power-law with upper and lower cutoffs of c_a^{-1} and $c_D \bar{y}$ respectively. Distributions of this form give rise to *anomalous scaling* in the moments, which we conjecture as the mechanism for Richards growth.

Demanding that $\bar{y}$ be the mean of this distribution implies the self-consistency condition

$$\bar{y} = \frac{\int y \rho(y) \, dy}{\int \rho(y) \, dy}. \quad (7)$$

By manipulating this condition [79], we arrive at a moment scaling relationship of

$$\langle y^2 \rangle \propto \langle y \rangle^{1 + \min(c_D - c_\mu, 1)}. \quad (8)$$

Thus, for $0 < c_D - c_\mu < 1$ we have that the second moment scales with the first moment as $\langle y^2 \rangle \sim \bar{y}^{1 + c_D - c_\mu}$, while for $c_D - c_\mu > 1$, we have a more typical scaling $\langle y^2 \rangle \sim \bar{y}^2$. This anomalous scaling *in steady state* is what motivated our hypothesis for Richards growth. However, absent a solution of the time-dependent Fokker-Planck equation, we cannot identify parameter regimes where the previous scaling holds away from steady state. As such, we introduce a seasonal model that allows us to take advantage of the results of this section.

A justification for employing the steady-state solution in a dynamic setting comes from the case of population decay for $\mu = 0$: If we take the scaling, $\langle y^2 \rangle \propto \langle y \rangle^{1 + \min(c_D, 1)}$, from the stationary state, and assume that it is maintained quasistatically during the decay process, we can make a prediction for the decay of the mean. In particular, $\partial_t \langle y \rangle = -a \langle y^2 \rangle \propto -\langle y \rangle^{1 + c_D}$, indicates that the mean should scale as t^{-1/c_D}. The numerical results, plotted in Fig. 2, indicate a power-law decay roughly consistent with this quasistatic approximation. A similar argument is made in Ref. [84] where power law decays as in Fig. 2 are demonstrated. To avoid problems with
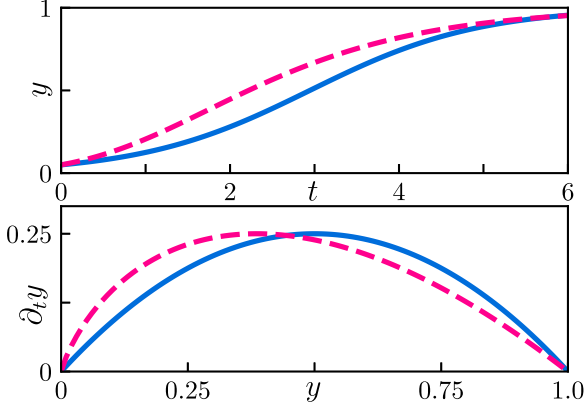
FIG. 1. Schematic illustration of a Richards versus logistic growth laws. The solid blue lines demonstrate a typical logistic growth curve, here with growth rate $\mu = 1$. The dashed red lines show a Richards growth curve, here with an exponent $\gamma = 1.1$, and a selected so that the saturation values are matched for illustrative purposes. Panel (a) shows the time courses for the two equations, and (b) shows how their growth rates change with population size. Notice how the inflection point in the Richards equation comes much earlier than that of the logistic equation.

the quasistatic assumption during growth, we next introduce a two-state model next that allows us to more controllably take advantage of this solution.

III. SEASONAL GROWTH MODEL

The combination of nonlinearity and stochasticity complicates the study of Eqs. (3) and (5). To simplify analysis while maintaining the qualitative features we believe to be responsible for the Richards form, we separate nonlinear growth and stochastic migration. To do so, we introduce a seasonal growth model composed of two distinct stages:

(1) *Exploration*. The exploration phase (season) has the population diffusing in the presence of seascape noise, as
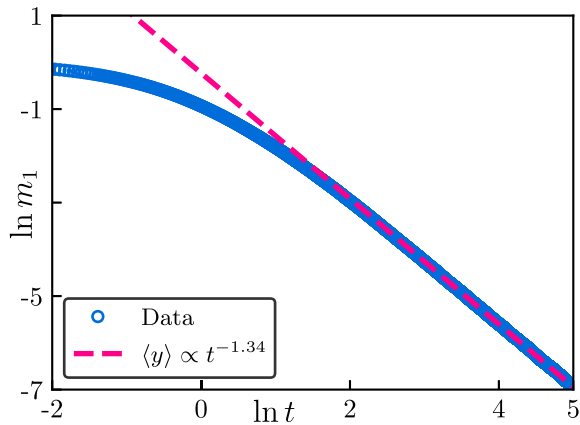

FIG. 2. Decay of mean-field model Eq. (5) in the case of $\mu = 0$. The blue circles show the numerically simulated decay of the mean, here with $a = 1$, $D = 0.8$, $\sigma^2 = 2$, $N = 2^{20}$, and $dt = 0.01$. The dashed red line shows a fitted power law to the tail of the decay. Notice that the fitted power law is around -1.34, and is slightly different than the predicted value of $-1/c_D = -1.25$.

described by

$$dy = D\nabla^2 y\,dt + \sigma y\,dW.$$

In the mean-field limit, $D\nabla^2 y$ is replaced by $D(\bar{y} - y)$, where $\bar{y} = \langle y \rangle$ at the start of the exploration phase. The exploration phase is run for a time T_e with $DT_e \gg 1$.

As these dynamics conserve the mean, $\bar{y}$ can be treated as a constant. In the absence of reproduction in the exploratory phase, a new interpretation for seascape noise is necessary. A potential cause is random extinctions of the populations at different locales and times. In this interpretation, the noise must have a negative mean, and $\langle y \rangle$ will decrease through the process. For a large enough population (to avoid the possibility of extinction) this overall loss can be restored in the subsequent growth stage, without qualitatively changing the results.

(2) *Growth*. Even when starting with a uniform distribution of numbers at each node, the stochasticity in the exploratory phase leads to a broad distribution of y_i at the end of this interval. In the subsequent growth phase, at each node we implement reproductive growth following the logistic equation,

$$\partial_t y_i = \mu y_i - a y_i^2,$$

for a short time T_g where $\mu T_g \ll 1$.

Equation (2) is deterministic, and can easily be solved to give the final population at each node in terms of the initial value. The exact form of the equation governing growth and saturation is not important, and as discussed in the following, any analytical form leads to similar results.

We alternate between exploration and growth for a large number of times (seasons) to generate trajectories for the moments of the population $m_n(t) = \langle y(t)^n \rangle$.

A. Stochastic exploration

In the exploration phase of the mean-field model, the distribution of y evolves according to the Fokker-Planck equation

$$\partial_t \rho = -\partial_y \left[D(\bar{y} - y) - \frac{\sigma^2}{2} \partial_y (y^2 \rho) \right]. \tag{9}$$

The stationary steady state solution is found by demanding a vanishing probability flux, and is proportional to

$$\rho(y) \propto e^{-c_D \bar{y}/y} y^{-2-c_D}, \tag{10}$$

which has the advertised structure of a power law with $c_D = 2D/\sigma^2$, and a lower cutoff set by $c_D \bar{y}$. Power laws arising from models with seascape noise are quite common, so this is well precedented [8,35,77,85–88]. However, the continuous variation of the exponent with the ratio c_D is unusual and likely a feature of the mean-field limit, though some similarly continuous nonuniversal exponents have also appeared in directed percolation under temporal disorder [89,90].

However, the steady state solution is only valid in the limit $T_e \to \infty$; for any finite T_e, the power-law tail will not extend to infinity, and higher moments will not diverge (see Appendix C). In addition, expansion and growth occur simultaneously in the original seascape Fisher equation, making the establishment of the full power-law tail implausible. Because of

this, we also impose an upper cutoff Λ to this distribution, simplifying it to

$$\rho(y) \propto y^{-2-c_D} \quad \text{for} \quad \Upsilon < y < \Lambda, \tag{11}$$

with $\rho(y) = 0$ otherwise. We have additionally imposed a lower cutoff Υ to ensure that the mean is equal to $\bar{y}$. For $0 < c_D < 1$, and as long as $\Lambda \gg \Upsilon$, the first moment of the distribution is given by

$$\langle y \rangle \approx \frac{1 + c_D}{c_D} \Upsilon, \tag{12}$$

setting the lower cutoff to

$$\Upsilon = \frac{c_D}{1 + c_D} \bar{y}. \tag{13}$$

The second moment is now given by

$$\langle y^2 \rangle \approx \frac{1 + c_D}{1 - c_D} \Lambda^{1-c_D} \Upsilon^{1+c_D} \propto \langle y \rangle^{1+c_D}. \tag{14}$$

We emphasize here the importance of spatial migration, as in its absence (by setting $D = 0$) the explicit dependence of the dynamics on $\bar{y}$ is removed. This removal disrupts the anomalous scaling of Eq. (14) and thus our proposed mechanism for Richards growth. While finding $\langle y \rangle$ in the case of $D = 0$ might be troublesome, here $\langle 1/y^m \rangle$ is exactly solvable for all integer $m \geqslant 1$, and will generically follow exponential trajectories in time.

B. Deterministic growth

Once the growth phase begins, the variable y_i's of nodes, distributed according to Eq. (11), serve as initial conditions for the logistic equation. For each node, the solution of the logistic equation gives

$$y_i(t) = \frac{e^{\mu t} \mu y_i}{a y_i (e^{\mu t} - 1) + \mu}. \tag{15}$$

Averaging over the initial conditions now leads to

$$\langle y(t) \rangle = \frac{\int_\Upsilon^\Lambda \frac{e^{\mu t} \mu y}{a y (e^{\mu t} - 1) + \mu} \rho(y) dy}{\int_\Upsilon^\Lambda \rho(y) dy}. \tag{16}$$

While this integral can be approximated in detail (see Appendix B), as long as the growth phase only occurs for a small time ($\mu T_g \ll 1$) we can expand our result for the mean at the end of the growth phase to $O(T_g)$ and find

$$\langle y(t + \Delta t) \rangle = (1 + \mu \Delta t) \langle y(t) \rangle - a \langle y^2(t) \rangle \Delta t. \tag{17}$$

If we take advantage of the fact that $\Lambda \gg \Upsilon$, then we can take advantage of the previously computed moments to obtain

$$\frac{\Delta \langle y(t) \rangle}{\Delta t} = \mu \langle y \rangle \left[1 - \frac{c_D}{1 - c_D} \frac{a\Lambda}{\mu} \left(\frac{c_D \langle y \rangle}{(1 + c_D)\Lambda} \right)^{c_D} \right]. \tag{18}$$

Therefore, when we write the dynamics of the mean in the growth phase, we have one term that scales as $\langle y \rangle$ and one term that scales as $\langle y \rangle^{1+c_D}$, leading to nonanalytic, Richards-like growth.

Upon iterating these dynamics at times $t_j = j(T_e + T_g)$, we find a population trajectory $m_1(t_j) = \langle y(t_j) \rangle$ governed by
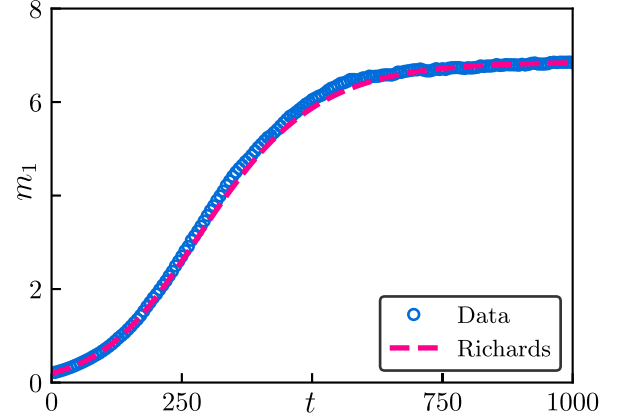

FIG. 3. Simulation of the seasonal growth model. Blue circles show the results of numerically solving the model over 175 cycles of exploration and growth for $N = 2^{20}$ nodes. The dashed line is a solution to the Richards equation with growth rate $\tilde{\mu}$ and exponent c_D as calculated in the main text, and with a numerically found carrying capacity. The simulation used $\mu = 1$, $a = 10^{-3}$, $\sigma = \sqrt{2}$, $D = 0.5$, $\Lambda = 500$, $T_g = 0.1$, and $T_e = 6$.

approximate Richards law to leading order in time and $\bar{y}/\Lambda$, of

$$\frac{dm_1(t)}{dt} = \tilde{\mu} m_1(t) - \tilde{a}(\Lambda) m_1(t)^{1+c_D} + O(m_1^2), \tag{19}$$

where $\tilde{\mu} = \frac{1}{1 + T_e/T_g} \mu$ is the effective growth rate and is cutoff independent. The carrying capacity is set by $\tilde{a}(\Lambda)$ which is some function of the cutoff and can be found numerically. We confirm these results in Fig. 3 where we see excellent agreement between the simulated mean population and the analytical prediction. We also note that the numerical results can also be reasonably fitted to a logistic sigmoid. However, what is significant is that models such as Eq. (3) contain the essential ingredients to analytically justify a Richards growth law.

IV. GENERAL CONSIDERATIONS

In this section we test the generality and applicability of the results from the seasonal model in a number of other contexts.

A. Dynamics of seascape mean field

In the seasonal model the nonanalytic form of Richards growth emerged from the power-law character of the distribution of local numbers, established from the combination of migration and seascape noise in the exploration phase. In the original model, and many likely realizations, growth and migration occur simultaneously, preventing formation of a well defined quasistationary power-law distribution. This complicated testing the foundation of our explanation of Richard's growth in terms of a relation between the growth exponent of the distributed population and its distribution among different locations.

To address these questions we simulated the full dynamics of Eq. (5) for $N = 2^{20}$ nodes. The mean, $\langle y \rangle = m_1$, of this distributed population grows in sigmoid fashion as depicted
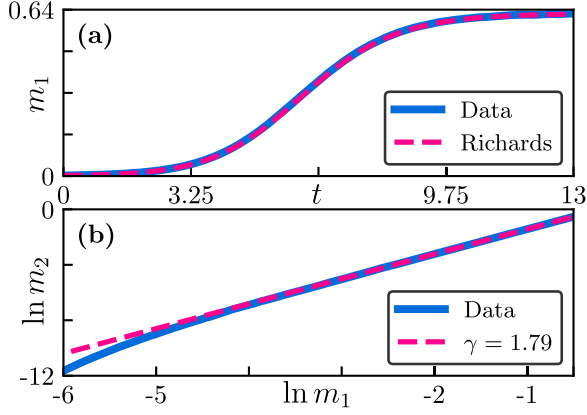
FIG. 4. Numerical simulation of the mean-field dynamics of Eq. (5), for $N = 2^{20}$ nodes with $\mu = a = 1$, $\sigma = \sqrt{2}$, $D = 1.2$, and $dt = 1/120$. The sigmoid curve in (a) is well fitted to a Richards equation with shape parameter $\gamma = 1.79$. (Only times after $4/\mu$ were used to fit the Richards exponent.) Panel (b) shows the relation between the first and second moments of the population on a log scale. The dashed line shows the best fit power law $m_2 \propto m_1{}^{\gamma}$.

in Fig. 4(a). In the absence of noise, with $\mu = a = 1$, the population would have saturated to $\mu/a = 1$; seascape noise reduces the saturation value to roughly 0.64. Allowing for a variable Richards growth exponent, the sigmoid curve is well fitted with a value of $\gamma = 1.79$. (Note that with the simultaneous action of growth and diffusion, we do not expect $\gamma = 1 + c_D$, with $c_D = 1.2$ for the chosen parameters of $\sigma^2 = 2$ and $D = 1.2$.)

Nonetheless, we can test whether something like our proposed mechanism is at work by plotting the time evolution of the second moment $\langle y^2 \rangle = m_2$ as a function of the first $\langle y \rangle = m_1$. As depicted in Fig. 4(b), at intermediate and late times, we find $m_2 \propto m_1{}^{\gamma}$ – a straight line in the log-log plot with a slope of $\gamma = 1.79$. Such log-log fits are a convenient way to retrieve the growth exponent γ in models such as these, and will be used throughout this paper. (The intercept for the log-log line is also useful, and related to the carrying capacity.)

Finding the first and second moments of a distributed population in a natural setting should be easier than characterizing the whole distribution. A relation such as $\langle y^2 \rangle \propto \langle y \rangle^{\gamma}$, coupled with a Richards fit to the growth curve of $\langle y \rangle$ with the same exponent would provide a good test of the proposed hypothesis.

B. Universality

The formulation of the model in terms of the logistic equation may give the impression that the obtained results are a consequence of its quadratic form. There are in fact many other analytic growth functions with saturation that generate sigmoid curves. The anomalous scaling, induced by the heavy-tailed distributions attributed to spatial diffusion and seascape noise, actually confers a universality to these results, independent of the assumed growth equation. Let us consider a generic *analytical* growth curve $g(y)$ with an initial growth rate μ that saturates to a carrying capacity $y = K$, which can

be written as

$$g(y) = \mu y \left(1 - \frac{y}{K} \right) f(y). \qquad (20)$$

The analytic function $f(y)$, with $f(0) = 1$, alters the growth away from the purely logistic case, and we will demand that $f(y) > 0$ for all y to ensure the only fixed points of the local growth are at $y = 0$ and $y = K$. This also guarantees that our local dynamics given $g(y)$ only have simple (nonrepeated) roots.

We will again demonstrate how such a generalized model behaves in the seasonal dynamics introduced before, where the population alternates dispersal with seascape noise, and local growth according to Eq. (20). As before, we restrict analysis to mean-field dispersion during the exploration phase, leading to

$$\begin{aligned} dy_i &= D(\bar{y} - y_i)dt + \sigma y dW_i(t), & \text{exploration} \\ dy_i &= \mu y_i (1 - y_i/K) f(y_i) dt, & \text{growth} \end{aligned}. \qquad (21)$$

The exploration phase is again assumed to be long enough to establish a power-law distribution for local numbers, as in Eq. (11). With the mean set by $\langle y \rangle = \bar{y} \propto \Upsilon$ (for $\Lambda \gg \Upsilon$), the higher moments behave as

$$\langle y^n \rangle \simeq \frac{\Lambda^{n-1-c_D}}{n-1-c_D} c_D \Upsilon^{1+c_D} \propto \Lambda^{n-1-c_D} \langle y \rangle^{1+c_D}. \qquad (22)$$

Notably, each higher moment has the same scaling with $\bar{y}$, although the prefactors vary by powers of the upper cutoff Λ.

Following a localized growth step of duration $\Delta t \ll \mu^{-1}$, the mean population is increased by $\Delta t \langle g(y) \rangle$. Since $g(y)$ can be expanded as a power series $g(y) = \mu y + g_2 y^2 + g_3 y^3 + \cdots$, we obtain

$$\langle g(y) \rangle = \mu \langle y \rangle - A(\Lambda) \langle y \rangle^{1+c_D} + \mathcal{O}(\langle y \rangle^2, \langle y \rangle^{2+c_D}). \qquad (23)$$

Once again, averaging over the exploration distribution establishes a Richards growth law; the difference with the purely logistic case is absorbed into the (cutoff dependent) coefficient of the nonanalytic saturation term. We test this universality by simulating seasonal growth with a quadratic $f(y)$ curve in Fig. 5.

C. Seascape Fisher equation in one and two dimensions

Armed with insights from the mean-field model, we now return to the seascape Fisher Eq. (3). To do so, we numerically simulate Eq. (3) using a central-difference discretization of the Laplacian on a lattice. We observe that the mean population can be well fit by a Richards curve, where the Richards exponent and carrying capacity are numerically determined from the data as in the mean-field case (Sec. IV A). As depicted in Fig. 6 this procedure leads to a characterization of the one dimensional growth with an emergent Richards shape parameter of $\gamma \approx 1.75$. The corresponding results in two dimensions (for a square lattice and periodic boundary conditions) are presented in Fig. 7 with shape parameter $\gamma \approx 1.71$. Here, we present these shape parameters as effective exponents describing particular simulations. Further investigation, possibly following Refs. [58,84,91] may shed light on the values of this exponent and its universality.
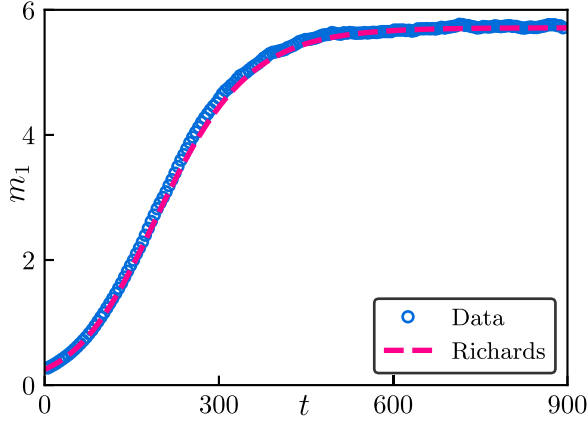
FIG. 5. Numerical simulation of seasonal growth dynamics with a deterministic phase of Eq. (20), with $f(y) = 1 + 0.2y/K + 0.3(y/K)^2$. The blue circles show the value of the average population at the end of each cycle, and the red dashed line shows the solution to Eq. (19) with $\tilde{\mu} = \frac{\mu}{1+T_e/T_g}$. We take the carrying capacity from the numerics in order to find $\tilde{a}(\Lambda)$. The simulation used $N = 2^{20}$, $\mu = 1$, $a = 10^{-3}$, $\sigma = \sqrt{2}$, $D = 0.6$, $\Lambda = 200$, $T_g = 0.1$, and $T_e = 5$.

D. Gompertz growth law for strong noise

We can rewrite Eq. (18) [see also Eq. (23)] as

$$\frac{\Delta \langle y(t) \rangle}{\Delta t} = \langle g(y) \rangle = \mu \langle y \rangle \left[1 - \left(\frac{\langle y \rangle}{K} \right)^{c_D} \right], \qquad (24)$$

in terms of a final capacity K. In the limit of strong seascape noise, we have $c_D = 2D/\sigma^2 \to 0$, and if we let $\mu = \tilde{\mu}/c_D$, then Eq. (24) acquires the form

$$\frac{\Delta \langle y(t) \rangle}{\Delta t} = -\tilde{\mu} \langle y \rangle \ln \left(\frac{\langle y \rangle}{K} \right). \qquad (25)$$

The above form, known as the *Gompertz equation*, is another commonly used growth law [1,2,13]. The qualitative predic-
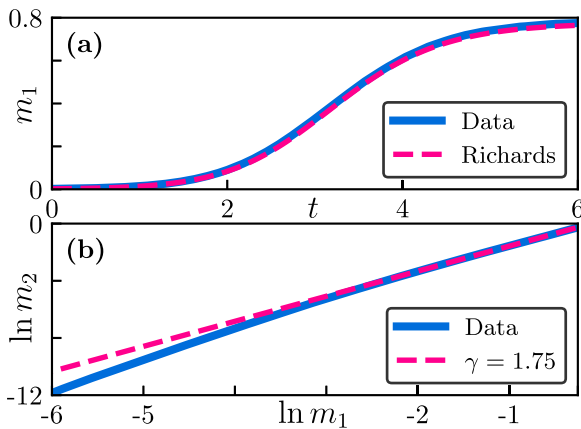

FIG. 6. Emergence of Richards growth in simulations of the seascape Fisher Eq. (3) in one dimension. Panel (a) compares the simulated first moment to the solution of a Richards equation, with a numerically fitted shape parameter γ. Panel (b) shows the relation between the first and second moments on a log scale. The dashed line shows the best fit power law $m_2 \propto m_2^\gamma$. We simulate $N = 2^{20}$ nodes with $\mu = a = D = 2$, $\sigma = \sqrt{2}$, and $dt = 1/200$. Only times after $4/\mu$ were used to fit the Richards exponent.
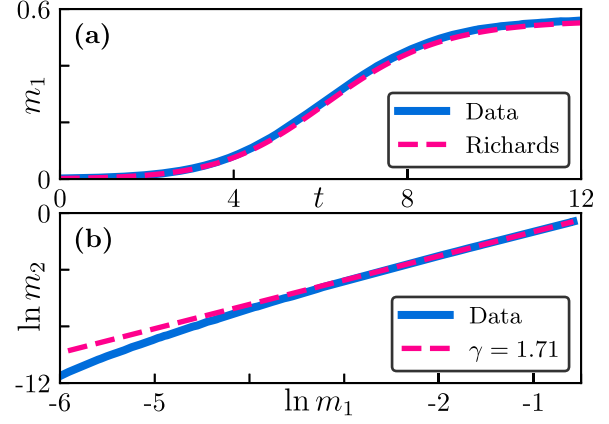

FIG. 7. Emergence of Richards growth in simulations of the seascape Fisher Eq. (3) in two dimensions. Panel (a) compares the simulated first moment to the solution to the Richards equation, with the shape parameter γ determined numerically. Panel (b) shows the relation between the first and second moments on a log scale. The dashed line show the best fit power law $m_2 \propto m_1^\gamma$. We simulate a grid of $2^{10} \times 2^{10}$ nodes with $\mu = a = D = 1$, $\sigma = 2$, and $dt = 1/100$. Only times after $4/\mu$ were used to fit the Richards exponent.

tion of the model is that the Gompertz law should emerge in systems subject to strong seascape noise.

V. DISCUSSION

Growth and saturation phenomena are prevalent in nature, necessitating a host of models and mathematical forms to quantify their description. The Richards and Gompertz laws stand prominently by providing successful empirical fits to sigmoid curves in diverse contexts [1,2,4,6,7,12–15,19–21,26]. A typical application involves data obtained by summing (averaging) numbers from a distributed data set. The appearance and success of such nonanalytical forms in describing sums is quite surprising: In the same sense that the probability distribution for the sum of many variables typically assumes the analytic Gaussian form, the most natural time evolution for the sum is an analytic growth law (whose first two terms form the logistic equation). A nonanalytic series (much like a critical exponent in critical phenomena) requires specific justification.

In this work, we argue that there is good theoretical and numerical evidence to suggest that Richards-like growth emerges as a natural consequence of the combination of dispersion and (seascape) stochasticity in a large distributed population. In steady state, the combination of the two establishes a broad power-law distribution at distinct locales; averaging any analytic growth rule with such a distribution leads to a nonanalytic Richards form. This argument, which nicely connects distribution of local numbers to the time evolution of the mean, however, relies on a form of quasistatic evolution that cannot be rigorously justified except in the case of a seasonal model that separates growth and stochastic dispersion. Fortunately, our numerical results in a number of cases other than the seasonal model suggest the broader applicability of this result. We further suggest a scheme (plotting

the second moment as a function of the mean) to test the validity of our proposed mechanism.

Several aspects of the model require further study: While the quasistatic arguments lead to a shape exponent of $\gamma = 1 + 2D/\sigma^2$, this is not the observed exponent even in the mean-field limit with a finite μ. The complexities of an evolving probability distribution invalidate the quasistatic result. It may be possible that a more delicate treatment of the Fokker-Planck equation can help identify an effective Richards exponent. The study of growth laws, or even statics, for the seascape Fisher equation in finite dimensions is also interesting, and may have connections to directed percolation [92] and directed polymers in random media [93,94].

While uniform initial conditions are amenable to analysis, the Fisher equation and its relatives are noted to have a number of interesting traveling wave solutions [28,32]. However, we are not aware of a study concerning the effect of seascape noise on the shape and speed of such wave fronts. And while we expect our results to hold true for some nonuniform initial distributions, the true limit of which conditions produce Richards-like growth is unexplored, and may include wave solutions. Such topics would require further study.

More complex connectivities are appropriate to social networks and spreading of contagions. Considering how the Richards equation has seen a recent rebirth in epidemiology and pandemic forecasting, it would be interesting to see whether implementing seascape growth on such human networks would generate relevant results. In particular, we may explore the role of long-range interactions which may be important to Richards growth [25,26].

While the most common modern use of the Richards equation is in epidemiology case studies, those tend to be out of the scope of laboratory testing. To test this mechanism *in vitro*, one avenue would be to use a bacterial population in a well mixed fluid as a controllable realization of the mean-field model. Perhaps local growth rates can be varied stochastically by application of randomized light sources. The prediction of the model is that upon increasing the strength of reproductive noise, the overall growth curve will change from logistic to Richards to Gompertz. However, practically measuring population in such a setup may be difficult, and the biochemical realities of bacterial growth may mean they would not follow logistic growth even in the absence of seascape noise.

It should be noted that our model does not necessarily apply to every situation where Gompertz or Richards laws have been found. While many real-world systems contain migration and seascape noise, we would not expect the mechanism to apply to settings such as tumor progression [2] or the growth profile of an individual plant [12–14], where Richards law has been invoked. It is therefore likely that there are other mechanisms that lead to the creation of Richards dynamics. However, the ingredients posed in this paper—migration plus seascape noise leading to power laws in moments—do indeed outline sufficient conditions for the presence of Richards growth curves.

APPENDIX A: NUMERICAL RECIPES

We describe here the numerical tools used to obtain the simulation results. The integration of stochastic equations is in general more difficult than the deterministic case. Deterministic ODEs can be treated with a variety of robust, accurate, and relatively simple methods, such as the fourth-order Runge-Kutta approach. In the stochastic case, we employ a method heavily inspired by that in Ref. [84]: The method we use involves splitting up the dynamics of the stochastic PDE,

$$dy = (\mu y - ay^2 + D\nabla^2 y)dt + \sigma y dW, \quad (A1)$$

into pieces which can be solved individually. We first treat the stochastic piece,

$$dy = \sigma y dW, \quad (A2)$$

whose solution, starting from any initial configuration $y(x, t)$, is a standard geometric Brownian motion,

$$y(x, t + dt) = y(x, t) \exp\left[-\frac{\sigma^2}{2}dt + \sigma dW(x, t)\right], \quad (A3)$$

with $dW(x, t) \sim N(0, dt)$. Using the output of the stochastic step we then use a standard Euler update rule,

$$y(x, t + dt) = y(x, t) + dtD\nabla^2 y(x, t), \quad (A4)$$

where $\nabla^2 y(x, t)$ is the appropriate discretization of the Laplacian on the given lattice. For mean field, $\nabla^2 y = \bar{y} - y$, while for a one dimensional lattice with unit spacing, $\nabla^2 y(x, t) = y(x + 1, t) + y(x - 1, t) - 2y(x, t)$. Finally, we take the output of this diffusion step and at each node apply a logistic growth, according to

$$y(x, t) = \frac{\mu e^{\mu t} y(x, 0)}{ay(x, 0)(e^{\mu t} - 1) + \mu}. \quad (A5)$$

For a more complicated growth dynamics, such as what is discussed in Sec. IV B, we will resort to using a routine Runge-Kutta solver, as implemented in MATLAB's ode45 function, to circumvent the lack of an available analytic solution. MATLAB implementations of all routines discussed can be found on GitHub [100].

APPENDIX B: SEASONAL GROWTH DYNAMICS

To analyze the dynamics of the seasonal model in Sec. III, it suffices to understand the dynamics of how the mean changes in a single growth phase. At the start of the phase, we assume a distribution of the form $\rho(y) \propto \hat{\rho}(y) = y^{-2-c_D}$ for $\Upsilon \leqslant y \leqslant \Lambda$, and 0 otherwise.

The evolution of each node during the growth phase follows a deterministic logistic growth. In particular, the population of a node after time T_g is given by

$$f(y; T_g) = \frac{y}{e^{-\mu T_g} + (1 - e^{-\mu T_g})(y/y_f)}, \quad (B1)$$

where $y_f = \mu/a$ is the saturation for logistic growth. The average population at the end of the growth phase is then

obtained as

$$\langle y(T_g)\rangle = \langle f(y; T_g)\rangle = \frac{\int f(y; T_g)\hat{\rho}(y)dy}{\int \hat{\rho}(y)dy}. \quad \text{(B2)}$$

Therefore,

$$\langle y(T_g)\rangle = \frac{(1+c_D)e^{\mu T_g}M^{-c_D}}{\Upsilon^{-1-c_D} - \Lambda^{-1-c_D}} \int_{M/\Lambda}^{M/\Upsilon} \frac{x^{c_D}}{x+1}dx, \quad \text{(B3)}$$

where we define $M = y_f/(e^{\mu T_g} - 1)$. It should be noted that there is not a particularly convenient closed form for the integral as presented. Moreover, since we assume $0 < c_D < 1$, the integral diverges as $(T_g)^{-c_D}$ for small times, meaning that it is sometimes more convenient to split the integral as $\int x^{c_D}/(x+1) = \int x^{c_D-1} - \int x^{c_D-1}/(x+1)$. For example, in the special case of $\Lambda \to \infty$, then this manipulation would become necessary, since the second integral would take on a term of $O(1)$ in time. This leads to an anomalous growth term, where $\langle y(t)\rangle - \langle y(0)\rangle \propto t^{c_D}$, which emphasizes the importance of the upper cutoff.

If Λ is finite, and we only care about first order in time, then we indeed can just take the expectation of both sides of the logistic growth equation and find

$$\frac{\langle y(T_g)\rangle - \langle y(0)\rangle}{T_g} = \mu\langle y(0)\rangle - a\langle y(0)^2\rangle + O(T_g). \quad \text{(B4)}$$

Expanding the relevant integrals gives

$$\frac{\Delta\langle y\rangle}{\Delta t} = \mu\Upsilon \frac{c_D + 1}{c_D} \frac{1 - (\Upsilon/\Lambda)^{c_D}}{1 - (\Upsilon/\Lambda)^{1+c_D}}$$
$$+ a\frac{c_D + 1}{c_D - 1} \frac{\Lambda^{1-c_D}}{\Upsilon^{-1-c_D}} \frac{1 - (\Upsilon/\Lambda)^{1-c_D}}{1 - (\Upsilon/\Lambda)^{1+c_D}}. \quad \text{(B5)}$$

Since $1 - c_D > 0$ and $\Lambda \gg \Upsilon$, we can trivially expand this out as

$$\frac{\Delta\langle y\rangle}{\Delta t} = \mu\Upsilon \frac{c_D + 1}{c_D}[1 - (\Upsilon/\Lambda)^{c_D}]$$
$$- a\frac{1 + c_D}{1 - c_D}\Lambda^{1-c_D}\Upsilon^{1+c_D}[1 - (\Upsilon/\Lambda)^{1-c_D}]$$
$$+ O[(\Upsilon/\Lambda)^{1+c_D}], \quad \text{(B6)}$$

which, if we neglect the higher order terms, returns us to Eq. (18). Therefore, a Richards-like growth law is retrieved.

If we are interested in the limit of small c_D, notice how the first term of the expansion has a term like $(1 - x^{c_D})/c_D$. Therefore, the limit becomes

$$\lim_{c_D \to 0^+} \frac{\Delta\langle y\rangle}{\Delta t} = \lim_{c_D \to 0^+} (\mu\langle y\rangle - a\langle y^2\rangle)$$
$$= -\mu\Upsilon \frac{\log(\Upsilon/\Lambda)}{1 - \Upsilon/\Lambda} - a\Lambda\Upsilon, \quad \text{(B7)}$$

which is difficult to rewrite in terms of $\langle y\rangle$ alone.

APPENDIX C: MOMENTS OF SEASCAPE DISPERSION

While not directly relevant to the study of scaling laws, for completeness we include a study of the dynamics of the moments, which can be used to determine relevant timescales for simulation. Let us consider a system under seascape noise and
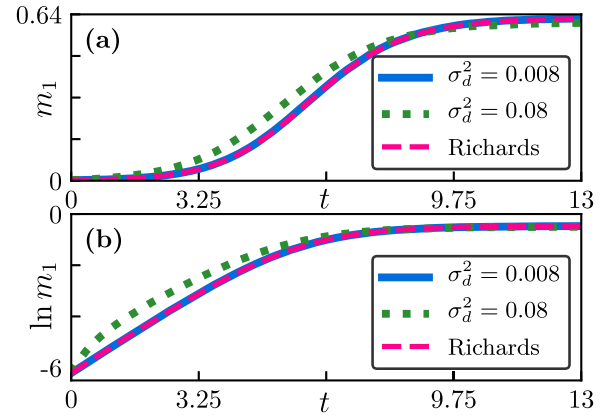

FIG. 8. Dynamics of the first moment $m_1 = \langle y\rangle$ using Eq. (D1) for various strengths of demographic noise. Panels (a) and (b) show the same data, but with alternate scales. Here we have $a = 1$, $D = 0.8$, $\sigma^2 = 2$, $y(x, t = 0) = 0.002$, $N = 2^{20}$, and $dt = 0.0125$. The solid blue line has $\sigma_d^2 = 0.008$, and the dotted green line has $\sigma_d^2 = 0.08$. The dashed red line reproduces the Richards curve from the $\sigma_d = 0$ case of Fig. 4. Notice how for small σ_d we match the Richards curve, but we get notable deflection in small y when σ_d is large.

dispersion, much like the exploratory phase of the seasonal model of Sec. III, with

$$dy = D(\bar{y} - y)dt + \sigma y dW. \quad \text{(C1)}$$

By applying Itô's lemma and taking the expectation of both sides, we get a set of ordinary differential equations of the form

$$\partial_t \langle y^m\rangle = A_m\langle y^{m-1}\rangle + B_m\langle y^m\rangle, \quad \text{(C2)}$$

with $A_m = mD\bar{y}$ and $B_m = m[(m-1)\sigma^2/2 - D]$. Note that each moment m depends only on itself and the moment $m - 1$, meaning that this is a solvable system. For example, because $\langle y(t)\rangle = \bar{y}$ for all time, this implies that the second moment is given by

$$\langle y^2(t)\rangle = \left(h_2 + \frac{2D\bar{y}^2}{\sigma^2 - 2D}\right)e^{(\sigma^2 - 2D)t} - \frac{2D\bar{y}^2}{\sigma^2 - 2D}, \quad \text{(C3)}$$

where $h_m \equiv \langle y^m(0)\rangle$, and assuming generic values of σ and D (such that the denominator is never 0). Notably, for $c_D = 2D/\sigma^2 < 1$, this means that the second moment grows exponentially. Given that the $(m-1)$th moment is known, the mth moment is given by

$$\langle y^m\rangle e^{-B_m t} = h_m + A_m \int_0^t e^{-B_m s}\langle y^{m-1}(s)\rangle ds. \quad \text{(C4)}$$

Assuming generic values of D and σ^2, this recursion relation is solved by something of the form

$$\langle y^m\rangle = \sum_{k=0}^m C_{m,k}e^{B_m t}. \quad \text{(C5)}$$

The coefficients $C_{m,k}$ can be solved for exactly using inductive methods, though such precision is mostly of specialized use. More importantly, this relation means that each moment above $m = 1$ experiences leading-order exponential growth, with a growth rate of $m[(m-1)\sigma^2/2 - D] > 0$ since $c_D < 1$.

Using this information, we can reasonably choose a befitting timescale for the exploration phase.

APPENDIX D: DEMOGRAPHIC NOISE

In many cases, it is natural to study the effects of demographic noise on spatially extended populations [79]. Such a consideration alters Eq. (3) with the addition of a term $\sigma_d\sqrt{y}dW'$ where dW' is a Brownian motion statistically independent of dW. The stochastic Fisher equation then becomes

$$dy = \mu y - ay^2 + D\nabla^2 y + \sigma y dW + \sigma_d \sqrt{y} dW'. \quad \text{(D1)}$$

The contribution due to demographic noise should become more important than that due to seascape noise as $y \to 0$. Comparing the final two terms in Eq. (D1) gives that de-

mographic noise should be the dominant contribution when $y < \sigma_d^2/\sigma^2$. Below this crossover threshold, the demographic noise destroys the anomalous scaling in the moments as in Eq. (14). Above this crossover threshold, we should have that the seascape noise dominates and our anomalous scaling (which provides the mechanism for Richards growth) will be restored. We test this numerically by simulating the mean-field limit of Eq. (D1) in Fig. 8, using the same conditions as in Fig. 4. When σ_d^2/σ^2 is substantially larger than the initial condition, then we get an initial altered growth phase that deflects it away from the $\sigma_d = 0$ curve. If the ratio is comparable or smaller to the current population, then growth proceeds similarly to the pure seascape case. In this paper we study growing populations and thus we ignore the contributions of demographic noise which will become negligible as the population becomes large.

[1] M. E. Turner Jr, E. L. Bradley Jr, K. A. Kirk, and K. M. Pruitt, Math. Biosci. **29**, 367 (1976).

[2] P. Gerlee, Cancer Res. **73**, 2407 (2013).

[3] C. P. Birch, Ann. Bot. **83**, 713 (1999).

[4] S. Y. Lee, B. Lei, and B. Mallick, PloS One **15**, e0236860 (2020).

[5] R. Claydon, S. Gartenstein, and A. T. Brown, arXiv:2106.12426.

[6] D. Fekedulegn, M. P. Mac Siurtain, and J. J. Colbert, Silva Fennica **33**, 327 (1999).

[7] X. Lifeng, S. Minggao, and W. Yuanjun, J. Biomath. **13**, 348 (1998).

[8] J. Desponds, A. Mayer, T. Mora, and A. M. Walczak, Population dynamics of immune repertoires, in *Mathematical, Computational and Experimental T Cell Immunology*, edited by C. Molina-Pars and G. Lythe (Springer, Cham, 2021).

[9] M. U. Gaimann, M. Nguyen, J. Desponds, and A. Mayer, Elife **9**, e61639 (2020).

[10] A. Amitai, L. Mesin, G. D. Victora, M. Kardar, and A. K. Chakraborty, Front. Microbiol. **8**, 1693 (2017).

[11] F. M. Burnet, Aust. J. Sci. **20**, 67 (1957).

[12] F. Richards, J. Exp. Bot. **10**, 290 (1959).

[13] A. Werker and K. Jaggard, Ann. Bot. **79**, 657 (1997).

[14] A. Gregorczyk, J. Agron. Crop Sci. **181**, 243 (1998).

[15] J. J. Pella and P. K. Tomlinson, Inter-Am. Trop. Tuna Comm. Bull. **13**, 416 (1969).

[16] K. Roosa, Y. Lee, R. Luo, A. Kirpich, R. Rothenberg, J. M. Hyman, P. Yan, and G. Chowell, J. Clin. Med. **9**, 596 (2020).

[17] K. Wu, D. Darcet, Q. Wang, and D. Sornette, Nonlinear Dyn. **101**, 1561 (2020).

[18] A. M. S. Macêdo, A. A. Brum, G. C. Duarte-Filho, F. A. G. Almeida, R. Ospina, and G. L. Vasconcelos, A comparative analysis between a SIRD compartmental model and the Richards growth model, *Trends in Computational and Applied Mathematics [online], 2021*, Vol. 22 (2022), pp. 545–557.

[19] M. Materassi, Chaos, Solitons Fractals: X **4**, 100032 (2019).

[20] P. Kumar, R. K. Singh, C. Nanda, H. Kalita, S. Patairiya, Y. D. Sharma, M. Rani, and A. S. Bhagavathula, medRxiv 2020.03.30.20047803 (2020).

[21] K. Roosa, Y. Lee, R. Luo, A. Kirpich, R. Rothenberg, J. Hyman, P. Yan, and G. b. Chowell, Infectious Dis. Model. **5**, 256 (2020).

[22] G. L. Vasconcelos, A. M. Macêdo, R. Ospina, F. A. Almeida, G. C. Duarte-Filho, A. A. Brum, and I. C. Souza, PeerJ **8**, e9421 (2020).

[23] F. Saif, medRxiv (2020), doi: 10.1101/2020.05.11.20098004.

[24] P.-F. Verhulst, Corresp. Math. Phys. **10**, 113 (1838).

[25] J. C. Mombach, N. Lemke, B. E. Bodmann, and M. A. P. Idiart, Europhys. Lett. **59**, 923 (2002).

[26] A. S. Martinez, R. S. González, and C. A. S. Terçariol, Physica A (Amsterdam, Neth.) **387**, 5679 (2008).

[27] X.-S. Wang, J. Wu, and Y. Yang, J. Theor. Biol. **313**, 12 (2012).

[28] R. Fisher, Ann. Eugenics **7**, 355 (1937).

[29] D. G. Aronson and H. F. Weinberger, Adv. Math. **30**, 33 (1978).

[30] S. A. Gourley, J. Math. Biol. **41**, 272 (2000).

[31] J. Kwapisz, J. Diff. Equ. **165**, 235 (2000).

[32] O. Hallatschek and K. S. Korolev, Phys. Rev. Lett. **103**, 108103 (2009).

[33] R. Durrett and S. Levin, Theor. Population Biol. **46**, 363 (1994).

[34] T. Butler and N. Goldenfeld, Phys. Rev. E **80**, 030902(R) (2009).

[35] O. Ovaskainen and B. Meerson, Trends Ecol. Evol. **25**, 643 (2010).

[36] A. Traulsen, J. C. Claussen, and C. Hauert, Phys. Rev. E **85**, 041901 (2012).

[37] G. W. Constable, T. Rogers, A. J. McKane, and C. E. Tarnita, Proc. Natl. Acad. Sci. U.S.A. **113**, E4745 (2016).

[38] H. Weissmann, N. M. Shnerb, and D. A. Kessler, Phys. Rev. E **98**, 022131 (2018).

[39] D. J. Merrell, *The Adaptive Seascape: The Mechanism of Evolution* (University of Minnesota Press, Minneapolis, 1994).

[40] V. Mustonen and M. Lässig, Trends Genet. **25**, 111 (2009).

[41] V. Mustonen and M. Lässig, Proc. Natl. Acad. Sci. U.S.A. **107**, 4248 (2010).

[42] A. Agarwala and D. S. Fisher, Theor. Population Biol. **130**, 13 (2019).

[43] S. Iram, E. Dolson, J. Chiel, J. Pelesko, N. Krishnan, Ö. Güngör, B. Kuznets-Speck, S. Deffner, E. Ilker, J. G. Scott *et al.*, Nat. Phys. **17**, 135 (2021).

[44] B. Trubenová, M. S. Krejca, P. K. Lehre, and T. Kötzing, Evolution **73**, 1356 (2019).

[45] S. Vincenzi, J. R. Soc., Interface **11**, 20140441 (2014).

[46] I. Cvijović, B. H. Good, E. R. Jerison, and M. M. Desai, Proc. Natl. Acad. Sci. U.S.A. **112**, E5021 (2015).

[47] S. Peischl and M. Kirkpatrick, Genetics **191**, 895 (2012).

[48] M. A. Muñoz, in *Advances in Condensed Matter and Statistical Physics*, edited by E. Korutcheva and R. Cuerno (Nova Science, New York, 2003), pp. 37–68.

[49] P. A. Moran, Aust. J. Zool. **1**, 291 (1953).

[50] P. Moran, Aust. J. Zool. **1**, 163 (1953).

[51] E. Ranta, V. Kaitala, J. Lindström, and E. Helle, Oikos **78**, 136 (1997).

[52] A. Liebhold, W. D. Koenig, and O. N. Bjørnstad, Annu. Rev. Ecol. Evol. Syst. **35**, 467 (2004).

[53] P. Ao, C. Kwon, and H. Qian, Complexity **12**, 19 (2007).

[54] Y. Tang, R. Yuan, J. Chen, and P. Ao, Phys. Rev. E **90**, 052121 (2014).

[55] C. Kwon and P. Ao, Phys. Rev. E **84**, 061106 (2011).

[56] G. Grinstein, M. A. Muñoz, and Y. Tu, Phys. Rev. Lett. **76**, 4376 (1996).

[57] Y. Tu, G. Grinstein, and M. A. Muñoz, Phys. Rev. Lett. **78**, 274 (1997).

[58] M. A. Muñoz and T. Hwa, Europhys. Lett. **41**, 147 (1998).

[59] H. Hinrichsen, Adv. Phys. **49**, 815 (2000).

[60] M. Kardar, G. Parisi, and Y.-C. Zhang, Phys. Rev. Lett. **56**, 889 (1986).

[61] M. Kardar and Y.-C. Zhang, Phys. Rev. Lett. **58**, 2087 (1987).

[62] B. Derrida, Physica A (Amsterdam, Neth.) **163**, 71 (1990).

[63] S. Chu and M. Kardar, Phys. Rev. E **94**, 010101(R) (2016).

[64] A. Borodin, I. Corwin, and P. Ferrari, Commun. Pure Appl. Math. **67**, 1129 (2014).

[65] E. Medina, T. Hwa, M. Kardar, and Y.-C. Zhang, Phys. Rev. A **39**, 3053 (1989).

[66] J. Quastel and H. Spohn, J. Stat. Phys. **160**, 965 (2015).

[67] T. Sasamoto and H. Spohn, Phys. Rev. Lett. **104**, 230602 (2010).

[68] T. Halpin-Healy, Phys. Rev. E **88**, 042118 (2013).

[69] C. Van den Broeck, J. M. R. Parrondo, J. Armero, and A. Hernández-Machado, Phys. Rev. E **49**, 2639 (1994).

[70] C. Van den Broeck, J. M. R. Parrondo, and R. Toral, Phys. Rev. Lett. **73**, 3395 (1994).

[71] C. Van den Broeck, J. M. R. Parrondo, R. Toral, and R. Kawai, Phys. Rev. E **55**, 4084 (1997).

[72] H. Hakoyama and Y. Iwasa, J. Theor. Biol. **232**, 203 (2005).

[73] A. Melbinger and M. Vergassola, Sci. Rep. **5**, 15211 (2015).

[74] S. Xu, S. Jiao, P. Jiang, and P. Ao, Phys. Rev. E **89**, 012724 (2014).

[75] M. T. Pearce, A. Agarwala, and D. S. Fisher, Proc. Natl. Acad. Sci. U.S.A. **117**, 14572 (2020).

[76] T. Chotibut, D. R. Nelson, and S. Succi, Physica A (Amsterdam, Neth.) **465**, 500 (2017).

[77] J. Desponds, T. Mora, and A. M. Walczak, Proc. Natl. Acad. Sci. U.S.A. **113**, 274 (2016).

[78] J.-P. Bouchaud and M. Mézard, Physica A (Amsterdam, Neth.) **282**, 536 (2000).

[79] B. Ottino-Löffler and M. Kardar, Phys. Rev. E **102**, 052106 (2020).

[80] P. Lombardo, A. Gambassi, and L. Dall'Asta, Phys. Rev. Lett. **112**, 148101 (2014).

[81] S. N. Gomes and G. A. Pavliotis, J. Nonlinear Sci. **28**, 905 (2018).

[82] Because $\bar{y}$ depends on the solution ρ, this makes the SDE (5) a McKean-Vlasov equation [95–99].

[83] M. A. Muñoz, F. Colaiori, and C. Castellano, Phys. Rev. E **72**, 056102 (2005).

[84] I. Dornic, H. Chaté, and M. A. Munoz, Phys. Rev. Lett. **94**, 100601 (2005).

[85] E. G. Leigh Jr, J. Theor. Biol. **90**, 213 (1981).

[86] R. Lande, Am. Nat. **142**, 911 (1993).

[87] H. Barghathi, S. Tackkett, and T. Vojta, Eur. Phys. J. B **90**, 129 (2017).

[88] P. Foley, Conserv. Biol. **8**, 124 (1994).

[89] I. Jensen, Phys. Rev. Lett. **77**, 4988 (1996).

[90] I. Jensen, J. Phys. A: Math. Gen. **38**, 1441 (2005).

[91] W. Genovese and M. A. Munoz, Phys. Rev. E **60**, 69 (1999).

[92] K. S. Korolev, M. Avlund, O. Hallatschek, and D. R. Nelson, Rev. Mod. Phys. **82**, 1691 (2010).

[93] F. Ginelli, V. Ahlers, R. Livi, D. Mukamel, A. Pikovsky, A. Politi, and A. Torcini, Phys. Rev. E **68**, 065102(R) (2003).

[94] S. E. Mangioni, R. R. Deza, R. Toral, and H. S. Wio, Phys. Rev. E **61**, 223 (2000).

[95] H. McKean Jr, Proc. Natl. Acad. Sci. U.S.A. **56**, 1907 (1966).

[96] A.-S. Sznitman, in *Ecole d'été de Probabilités de Saint-Flour XIX-1989* (Springer, Berlin, New York, 1991), pp. 165–251.

[97] C. Graham, Stochastic Processes Appl. **40**, 69 (1992).

[98] M. A. Mezerdi, K. Bahlali, N. Khelfallah, and B. Mezerdi, arXiv:1909.13699.

[99] Y. S. Mishura and A. Y. Veretennikov, Theor. Probab. Math. Statist. **103**, 59 (2020).

[100] https://github.com/dancewartz/RichardsGrowth.